Minghua Zheng[1*], Luca Delle Monache[1], Xingren Wu[2], Brian Kawzenuk[1], F. Martin Ralph[1], Yanqiu Zhu[3], Ryan Torn[4], Vijay S. Tallapragada[5], Zhenhai Zhang[1], Keqin Wu[2]

[1] Center for Western Weather and Water Extremes, Scripps Institution of Oceanography, University of California San Diego, La Jolla, California

[2] I. M. Systems Group Inc. at National Oceanic and Atmospheric Administration (NOAA) National Centers for Environmental Prediction (NCEP)/ Environmental Modeling Center (EMC), College Park, Maryland

[3] National Aeronautics and Space Administration(NASA)/Goddard Space Flight Center (GSFC), Greenbelt, Maryland

[4] University at Albany, State University of New York, Albany, New York

[5] NOAA NCEP / EMC, College Park, Maryland

[*]Corresponding author: Name: Minghua Zheng, Email: `mzheng@ucsd.edu`, Tel: +1 858-534-1819.

Key Points:

- Dropsonde data can lead to an increase of 5-10% in the amount of tropospheric radiance for the operational data assimilation system.

- The assimilation of dropsonde data results in reduced total bias corrections for radiance data needed by modeling systems to use radiances.

- Positive impacts of dropsondes on radiances assimilation lasted for ~1 week after the last mission of 2020 Atmospheric River Reconnaissance.

Abstract

Satellites provide the primary dataset for monitoring the earth system and constraining analyses in numerical models. A challenge for utilizing satellite radiances is the estimation of their biases. High-accuracy non-radiance data are typically employed to anchor radiance bias corrections. This study provides the first assessment of impacts of dropsonde data collected during the Atmospheric River (AR) Reconnaissance program that samples ARs over the Northeast Pacific on the radiance assimilation using the Global Forecast System (GFS) and the Global Data Assimilation System. Including this dropsonde dataset has provided better anchoring for bias corrections and improved model background, leading to an increase of ~5-10% in the amount of assimilated microwave radiance in the lower/middle troposphere over the Northeast Pacific and North America. The impact on tropospheric infrared radiance is small but also beneficial. This result points to the usefulness of dropsondes, along with other conventional data, in the assimilation of satellite radiance.

Plain Language Summary

Large biases impact the assimilation of satellite radiances. More accurate observations from other observing platforms are employed to reduce systematic biases

in model analyses. This research provides the first evaluation of the impact of dropsondes on the assimilation of radiances. Dropsonde data were collected during the 2020 Atmospheric River Reconnaissance (AR Recon). With the U.S. Global Forecast System and the Global Data Assimilation System, we found that dropsondes improve the model prediction and help with radiance bias estimates, leading to an increase of ~5-10% in the number of microwave radiance in the lower- to middle- troposphere over the northeastern Pacific and North America. Small but positive impacts are also found in tropospheric infrared radiance. This research suggests that AR Recon dropsondes increase the number of radiance for assimilation, and in future observing networks could be considered as anchor data to help with the assimilation of satellite data over data-sparse areas.

1 Introduction

Satellite observations have been a primary dataset for monitoring and modeling the atmosphere, the land surface, and the oceans (Rao et al., 1990; Andersson et al., 2005; Posselt et al., 2008; Maier et al., 2021). Some of the largest improvements in forecast skill at operational numerical weather prediction (NWP) centers were associated with either the newly available satellite radiance (McNally et al., 2006; Boukabara et al., 2007; Bormann et al., 2013; Eresmaa et al., 2017) or the development of new data assimilation techniques for radiances (Courtier et al., 1993; Eyre et al., 1993; Caplan et al., 1997; Bauer et al., 2006; Geer and Bauer 2011; Zhu et al., 2014a). Proper bias correction is essential for making optimal use of satellite radiances (Harris and Kelly, 2001; Dee, 2004; Auligné et al., 2007; Dee and Uppala, 2009; Zhu et al., 2014a; Otkin et al., 2018). Satellite data can have systematic biases that depend on the sensors, scan angle, calibrations, latitudes, and seasonality (e.g., Dee, 2004; Li et al., 2019). Additionally, NWP models used for radiance assimilation can have systematic errors that stem from imperfect model dynamics, physics, and initial conditions (e.g., Bhargava et al., 2018; Zheng et al., 2019). Lastly, approximations in the radiative transfer model can introduce state-dependent biases (e.g., Weng, 2007). Estimating radiance biases has been challenging because the observation bias is inseparable from the model bias due to unknown truth. Most operational centers (e.g., the National Centers for Environmental Prediction (NCEP)) employ variational bias correction schemes (Derber and Wu, 1998), which assume models to be unbiased. However, since forecast models have biases, independent observation types with small or negligible biases, referred to as the "anchor data", are required to prevent the analysis from drifting to systematic model biases and underutilizing satellite data (e.g., Cucurull et al., 2014). It is still unclear what impact most anchor data have on radiance assimilation and how effective a model can respond to aditional anchor data.

While there have been a few studies on the anchoring effect of radio occultation (RO) data on stratospheric satellite channels (Healy, 2008; Cucurull et al., 2014), no study to date has examined the anchoring impact of conventional observations (e.g., radiosonde data). In this study, we have investigated the role of

reconnaissance dropsonde data in affecting the assimilation of satellite radiance data. We are particularly interested in the dropsondes collected during the Atmospheric River (AR) Reconnaissance (AR Recon; Lavers et al., 2018; Ralph et al., 2020; Zheng et al., 2021a) field campaign (e.g., Majumdar, 2016) that aims to enhance the upstream sampling of landfalling ARs (Zhu and Newell, 1994; Ralph et al., 2004, 2005, 2017; Guan and Waliser, 2015; Gershunov et al., 2017; Reynolds et al., 2019; Zhang et al., 2019) in the Northeast Pacific in an effort to improve forecast skill over the US West Coast at 1-5 day lead times. Overall positive impact from aircraft dropsondes have been documented in the literature (e.g., Pu et al., 2008). Recent studies demonstrated the positive impact from AR Recon dropsondes data through both Forecast Sensitivity and Observation Impact (FSOI) studies and the full data denial experiments (Stone et al, 2020; Zheng et al., 2021b).

Over the ocean, satellite radiance is the primary observational dataset used for informing and updating model initial conditions; however, only a few observation types are available to anchor radiance assimilation (Hersbach et al., 2020). Data gaps identified in and around ARs (Zheng et al., 2021a) result in a substantial reduction in the availability of anchoring data compared to non-AR regions and indicate that AR Recon data could provide critical anchor data. Cucurull et al. (2014) demonstrated the ability of the unbiased spaceborne RO data to improve the bias correction of satellite radiances based on the NCEP Gridpoint Statistical Interpolation (GSI, Kleist et al., 2009) data assimilation system. However, both the quality and quantity of the RO data are degraded toward the lower troposphere, resulting in a limited impact on constraining model analyses in lower levels. In contrast, the high-quality and high-vertical-resolution dropsonde data have great potential to anchor lower-level satellite channels (i.e., surface and cloud-sensitive) because they represent direct observations from near the ocean surface to the upper troposphere in all-weather conditions.

The objective of this study is to investigate the ability of AR Recon data to influence radiance assimilation in Finite-Volume Cubed-sphere dynamical core (FV3)-based Global Forecast System (GFS, Chen et al., 2019) and the corresponding Global Data Assimilation System (GDAS) at NCEP. This study offers the first systematic analysis on the anchoring effect of AR Recon dropsondes for two representative satellite radiance types: 1) microwave soundings, 2) hyperspectral infrared soundings. Data denial experiments were designed with the FV3GFS/GDAS for 2020 AR Recon dropsonde data. The differences between available radiances in experiments with and without AR Recon data over the northeastern Pacific and North America (PNA) are explored, as well as the mechanisms behind the impact of this data on radiance assimilation.

2 Data and Methodology

2.1 Experiment set-up

In this study, we have employed GFS version 15 (Yang and Tallapragada, 2018)

developed at NCEP and the corresponding GDAS to perform data denial experiments for AR Recon dropsonde data. The GFS maintains a horizontal resolution of ~13 km and has 64 levels in the vertical with a model top of 0.2 hPa. A hybrid 4-dimensional ensemble-variational (Wang and Lei, 2014; Kleist and Ide, 2015) method was used in GDAS to assimilate observational data. The 80 ensemble member inputs have a horizontal resolution of ~25 km. GDAS is cycled four times daily (00, 06, 12, and 18 UTC) with an observational window of ±3 hours around each analysis time. The background fields are based on a 9-hour forecast from the previous cycle. Data types used in the data denial experiments are shown in Table S1.

The experiments run from 0000 UTC 24 January 2020 to 0000 UTC 18 March 2020 and cover 17 AR Recon Intensive Observation Periods (IOPs, Table S2). The GFS/GDAS was run parallelly with two sets of analyses: 1) control runs called "Ctrl" that assimilated AR Recon dropsonde data and other routine observations (Table S1), 2) denial runs called "Deny" that assimilated the same set of observations as Ctrl but withholding the AR Recon dropsonde data. The satellite radiances for GDAS were used for this study, and differences in Ctrl and Deny have been examined. We used the Advanced Microwave Sounding Unit-A (AMSU-A, Rosenkranz, 2001; Mo, 2011) onboard the NOAA-19 satellite and the Cross-track Infrared Sounder (CrIS, Han et al., 2013) onboard NOAA-20 as representative radiances for the microwave sounding and the hyperspectral infrared sounder, respectively. The positive impact of AMSU-A data has been demonstrated in literature (e.g., Boukabara et al., 2007; Liu et al., 2012), and its bias corrections are sensitive to RO data (Cucurull et al. 2014). CrIS has been chosen to represent the infrared radiance because it has a beneficial impact on scales from nowcasting to the medium range (Eresmaa et al., 2017), and the impact is also sensitive to bias correction algorithms (Li et al., 2019). Figure 1 shows a snapshot of the AMSU-A channel 1 (weighting function,WF peaks at the surface) and CrIS channel 85 (WF peaks at the 265 hPa) radiance distribution for the 6-h assimilation window centered at 0000 UTC 4 February.
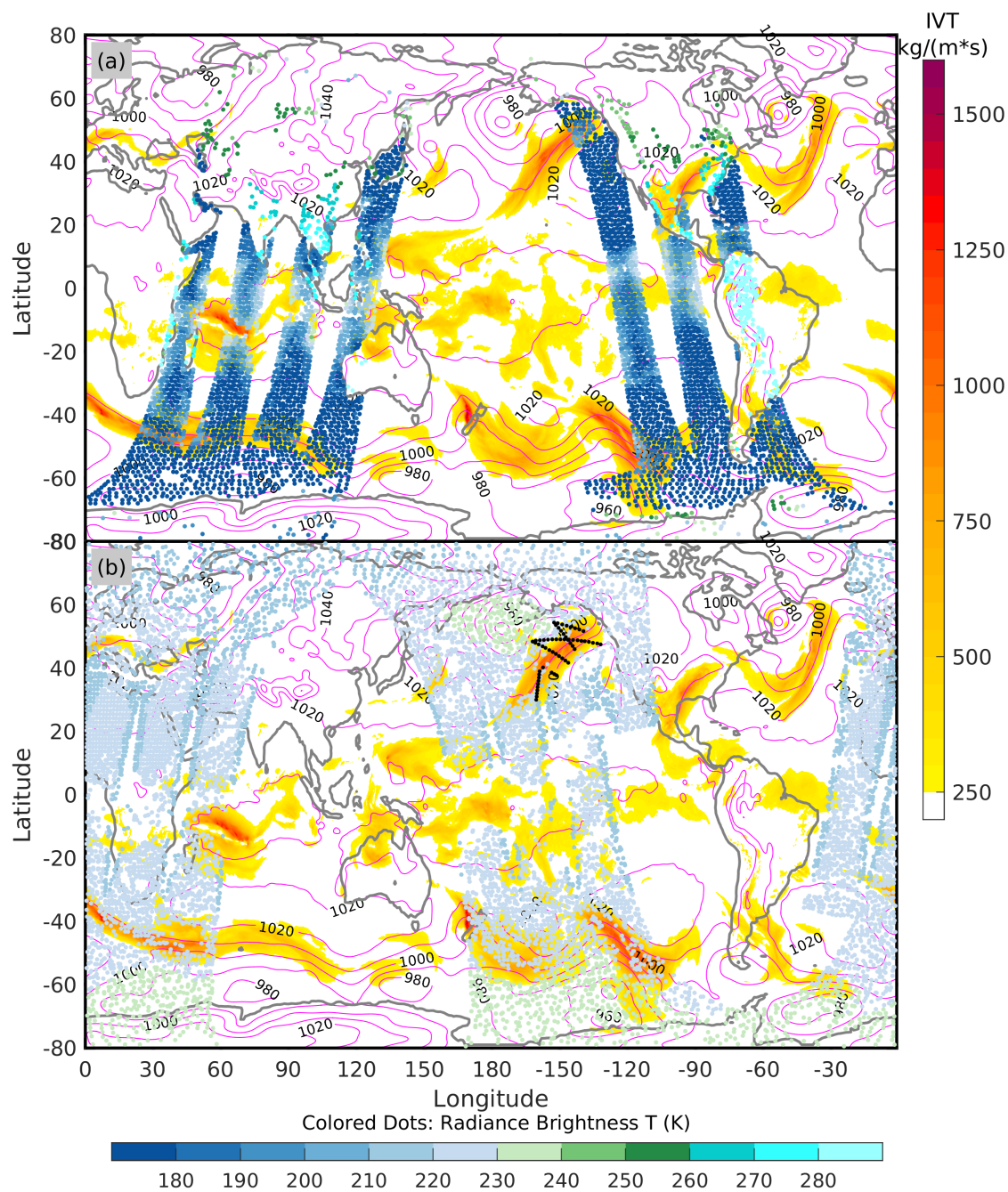
Figure 1 A snapshot of two types of satellite radiance assimilated in the 6-h time window centered at 0000 UTC 4 February 2020 from the Ctrl experiment. (a) AMSU-A channel 1 onboard NOAA-19; (b) CrIS channel 85 onboard NOAA-20. Colored dots are the raw brightness temperature [K] for each radiance data. The yellow-orange-red shaded are the IVT amplitude [kg m^{-1} s^{-1}] in the GFS Final Analysis (FNL). Black dots in (b) correspond to locations of assimilated dropsondes, while the magenta isolines indicate the FNL mean seal level pressure [hPa].

2.2 Radiance bias-correction scheme in GSI

The original NCEP radiance bias correction was a two-step process that included a scan-angle component and a variational air-mass component (Derber and Wu, 1998). The observation operator $\tilde{h}$ in the original scheme can be expressed as follows:

$$\tilde{h}\left(\mathrm{x},\,\beta\right) = h(\mathrm{x}) + b^{\mathrm{air}}\left(\mathbf{x}, \beta\right) + b^{\mathrm{angle}}, \quad (1)$$

where $\mathbf{x}$ represents the model state vector; β is the bias correction coefficient, and $h(\mathrm{x})$ represents the radiative transfer for the radiance of interest. The scan-angle component is represented by b^{angle} and is calculated outside the GSI. The variational air-mass component $b^{\mathrm{air}}\left(\mathbf{x}, \beta\right)$ is updated inside the GSI and is expressed as a linear combination of N predictors. The original scheme consists of five predictors, which are the global offset, the zenith angle predictor, the cloud liquid water (CLW) term, temperature lapse rate predictor, and the square of the lapse rate.

Zhu et al. (2014a) introduced the enhanced radiance bias correction scheme to the NCEP GSI, in which the scan-angle component is incorporated into GSI and is expressed as:

$$b^{\mathrm{angle}} = \sum_{k=1}^{K} \beta_{N+k}\phi^k, \quad (2)$$

where b^{angle} is a K-th-order polynomial of scan angle ϕ. K is typically chosen as 3 or 4. Note that the original zenith angle predictor is no longer needed in the enhanced scheme. Therefore, the observation operator $\tilde{h}$ is updated with the use of equation (2) and can be expressed as:

$$\tilde{h}\left(\mathbf{x}, \beta\right) = h\left(\mathbf{x}\right) + \sum_{k=1}^{N+K-1} \beta_k p_k(\mathbf{x}), \quad (3)$$

where p_k represents a set of predictors with $k = 1, 2, …, N+K\text{-}1$ and $p_1 = 1$. The coefficients are estimated along with $\mathbf{x}$ during the minimization of the cost function $J\left(\mathbf{x}, \beta\right)$.

The follow-up study by Zhu et al. (2014b) applied a new emissivity sensitivity predictor to GSI to account for the land/sea contrasts. With the development of all-sky radiance assimilation, the CLW predictor term was removed (Zhu et al., 2016).

3 Results

3.1 Microwave soundings

3.1.1 All-sky radiance

Channel 1 of AMSU-A onboard NOAA-19 has been chosen to represent all-sky microwave radiances assimilated by the GDAS. First, the PNA region is defined as from 40°W-180°W and 20°N-75°N, and the radiance observations that passed quality control (QC) in GDAS within the PNA region are counted and investigated. Radiance counts that can pass the QC are mainly impacted by the observation minus model background departures (OmB) and the bias correction applied to reduce the OmB. Therefore, we have examined the difference in OmB and in the total bias correction (TBC) to futher explore how the assimilation of dropsondes change these metrics.

The number of QC-ed radiance for the AMSU-A channel 1 varies from ~500–900 over the PNA region due to the satellite's sun-synchronous orbit (Fig. 2a). No significant differences are seen in the first two weeks of the investigated period (Fig. 2b). Slightly more radiance data (e.g., 0.3%) is seen in Ctrl than in Deny from February 8-28 (Fig. 2b). The amount of radiance data in Ctrl significantly exceeds that in Deny since March 1, with the percentage of increase reaching the peak value (i.e., 7.4%) on March 9 (IOP 15). After the last IOP (IOP 17) on March 11, the positive difference in Ctrl and Deny drops rapidly (Fig. 2b).

Figure 2c compares the differences between Ctrl and Deny in the standard deviation (STD) of OMB for the brightness temperature. The difference between Ctrl and Deny in the OmB STD is steadily trending negatively from February 8 to March 10 and trends back toward zero after the last AR Recon IOP (Figs. 2d). The assimilation of dropsondes overall reduces the OmB variation before performing bias corrections (Figs. 2c-d). This indicates that dropsondes have improved the model background, likely due to an improvement in model initial conditions, and the improvement maximizes toward the end of the AR Recon period.
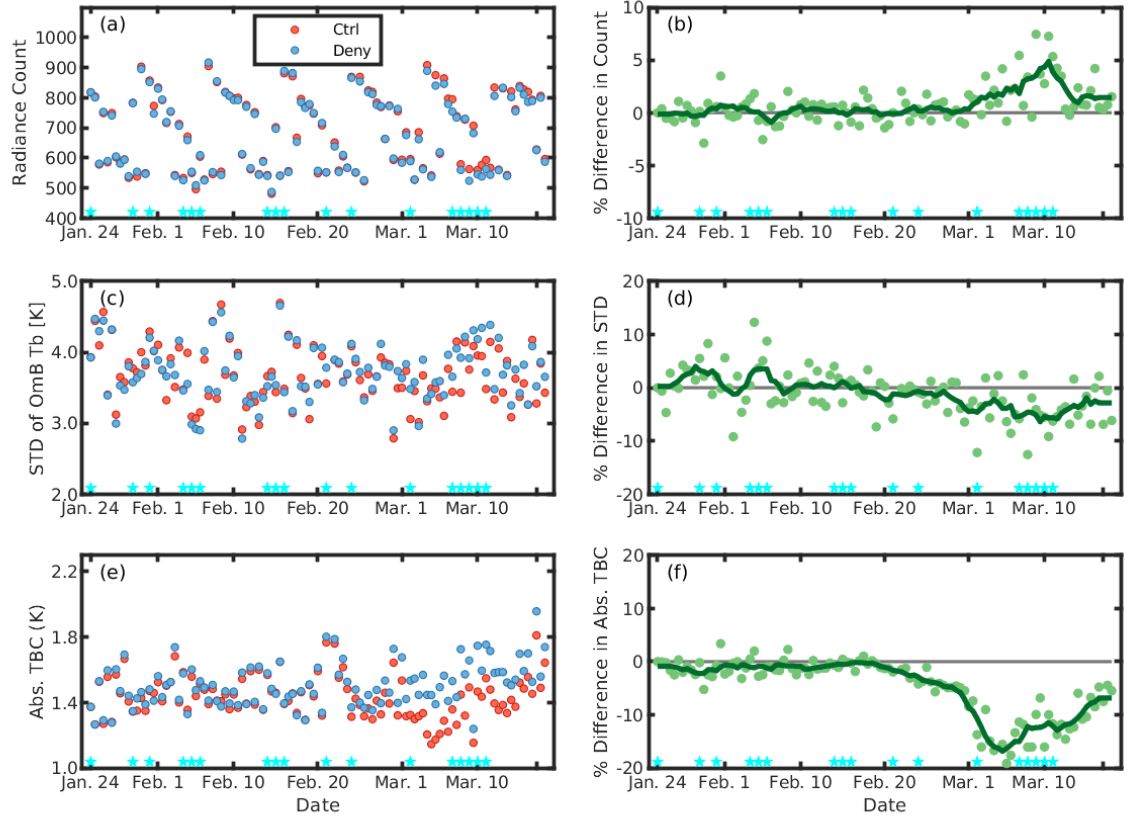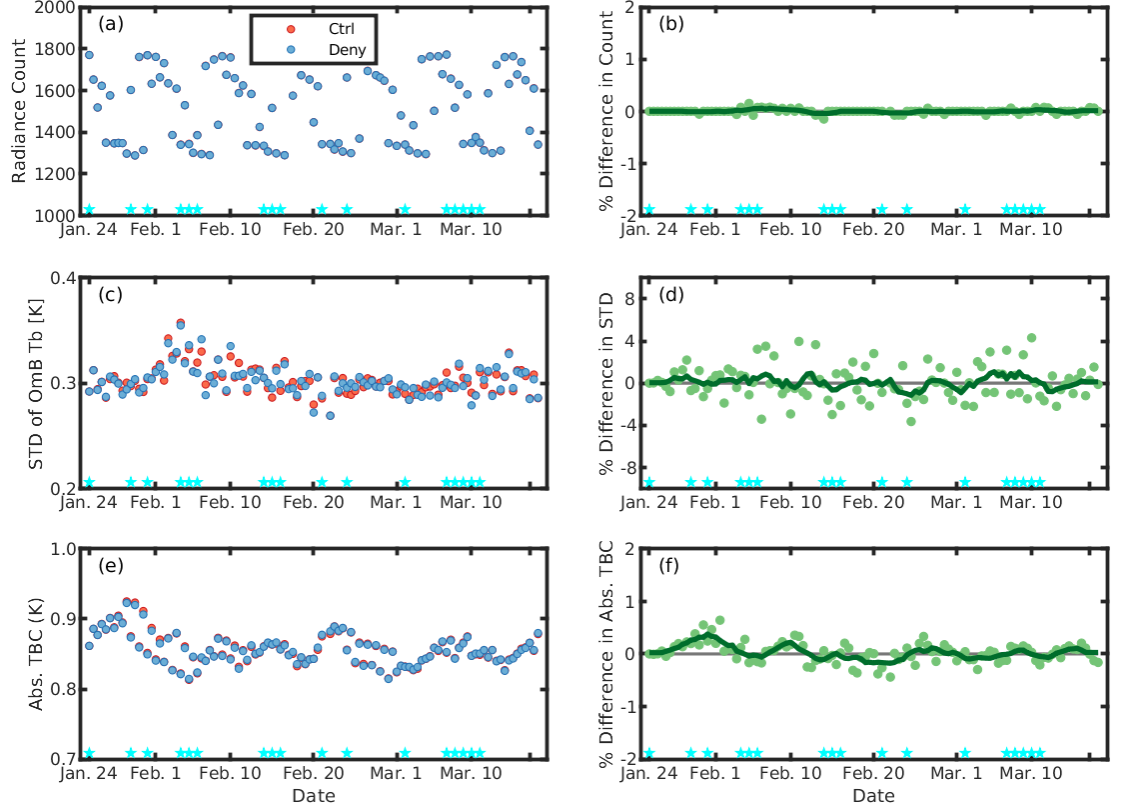
Figure 2. Statistics of AMSU-A channel 1 radiance observations that passed the QC over the PNA region in GDAS for the Ctrl and Deny runs from January 24 to March 18, 2020. (a) radiance counts in Ctrl and Deny, (b) % of radiance count change (green dots) in Ctrl w.r.t. Deny, and the 7-point running mean (dark green line); (c) standard deviation (STD, [K]) for OmB in Ctrl and Deny; (d) % of STD change in Ctrl w.r.t. Deny; (e) absolute value of TBC (Abs. TBC, [K]) in Ctrl and Deny; (f) % of Abs. TBC change in Ctrl w.r.t. Deny. Each dot represents data from a 6-hour data assimilation window centered at 0000 UTC or 1200 UTC. Cyan stars at the bottom of each panel denote 17 AR Recon IOPs (Table S2).

TBCs have been acknowledged to impact the assimilated radiance data (Cucurull et al., 2014). We further investigated the differences in the absolute value of the TBC for the two experiments. The TBC amplitude for Ctrl is smaller than for Deny beyond February 20, reaching a maximum percentage change of ~15-20% during the last AR Recon sequence flight (Figs. 2e-f).

To determine the relationship between radiance counts and the above two met-

rics, the partial correlation (Stuart et al., 2004) between radiance count change and each metric withholding the contribution from the other metric was calculated. The partial correlation between the percentage change of TBC amplitude in Ctrl and that of the radiance count change is -0.27 (significant at 99% student t-test level) while the similar metric for STD and the radiance count change is -0.19 (significant at 95% student t-test level). Consistent results are found for the similar satellite channel over the Northern Hemisphere (Fig. S1), for other all-sky channels (e.g., channel 15 shown in Fig. S2), and for the assimilated data (after assimilation, Fig. S3). These results suggest that with better anchor data from dropsondes, the amplitude of bias corrections needed for all-sky microwave radiances is reduced significantly, which is the dominant factor for increased radiance data in Ctrl. The improved model background in low levels from the assimilation of dropsondes also allows more radiance to pass the QC.

To investigate the duration of impact that dropsondes have, 17 data points from March 10 (IOP 16) through March 18 (end of both experiments) were used to calculate linear regressions. Differences in two experiments are diminished after 8.4 days for radiance count, 11.7 days for the OMB STD, and 13.0 for the TBC amplitude after the last dropsondes were deployed. This estimation implies that it takes 1-2 weeks for the modeling system to repond to the addition or removal of dropsonde anchor data.

Figure

3. Same as Fig. 2 but for channel 9 (WF peaks at ~86 hPa).

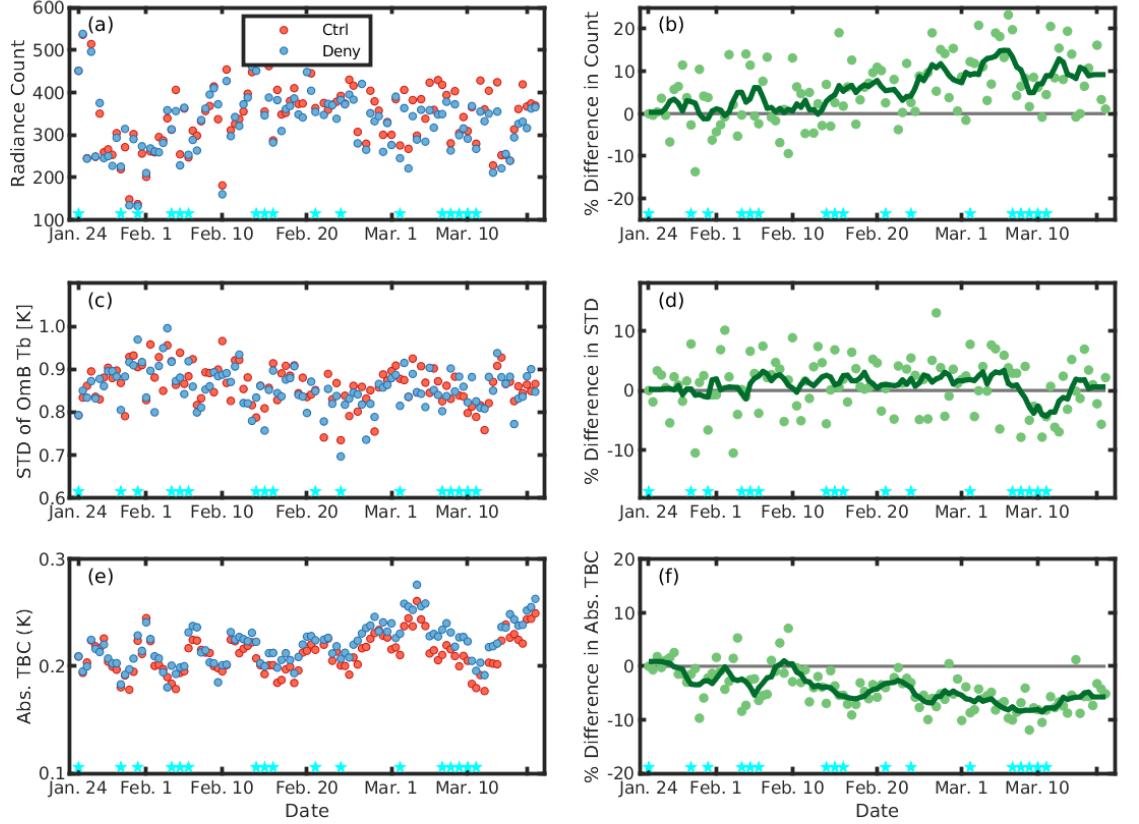### 3.1.2 Lower stratospheric channels

Channels 9-14 of AMSU-A are upper-level channels with weighting functions peaking in the stratosphere (Fig. S4). The number of radiance data for channel 9 that can pass the QC is twice (Fig. 3a) of that of the all-sky radiance channel. The Deny and Ctrl do not show any significant differences in the radiance count, with a maximum difference count of only 2. The two metrics (STD of OMB and TBC amplitude) for the two experiments show no clear trends nor significant differences, albeit small fluctuations around zero do exist beyond the first five days (Figs. 3d, f). These results suggest that the anchoring impact of dropsondes in the lower stratosphere is insignificant. Consistent results are found employing other stratospheric channels from AMSU-A (not shown) and other microwave soundings (e.g., the ATM aboard NOAA-20, Fig. S5).

3.2 Hyperspectral infrared sounders

Infrared radiances have been providing the largest amount of radiance data in the GFS/GDAS since they became operational and have been demonstrated to

10

improve the forecast skill particularly when using the total impact metrics (Ota et al., 2013). We have examined the anchoring impact of dropsonde data on the representative operational hyperspectral infrared sounders, including the CrIS (Han et al., 2013), Infrared Atmospheric Sounding Interferometer (IASI, Collard, 2007; Hilton et al., 2009), and Atmospheric Infrared Sounder (AIRS, Aumann et al., 2003; McNally et al., 2006). Examination of the CrIS radiance onboard NOAA-20 that was launched in November 2017, including 1305 channels (GDAS has used 399 of them, Gambacorta and Barne, 2013) that cover three spectral bands, short-wave IR (SWIR), mid-wave IR (MWIR), and long-wave IR (LWIR), is of particular interest to this study. CrIS channel 1022 is a representative MWIR channel with WF peaking at 585 hPa. The number of the radiance from this channel is only 200-500 per analysis time over the PNA region likely due to the removal of cloud-affected pixels (Fig. 4). The radiance change in Ctrl shows an increasing trend from February 10 with a peak increase of ~20% from March 6-7. However, the OmB STD change does not show a corresponding negative trend, except for significant negative values from March 7-11. The correlation between the radiance count change and the OmB std change is weakly positive. In contrast, the TBC amplitude is negatively correlated with the radiance count change at the significant level of 99.9%, suggesting that the impact of dropsonde data on radiance counts is mainly achieved through the reduced TBC amplitude. The anchoring impact on infrared radiance data is more rapidly reflected than that on the all-sky radiance data.

A representative LWIR channel (i.e., channel 85) that peaks in the upper troposphere (i.e., ~235 hPa) is also investigated (Fig. S6). Both the STD of OmB and the amplitude of TBC are smaller (< 0.2 K) for the LWIR channel than those for the MWIR channel, and the two experiments don't show a significant difference for either metrics, despite a small increase ($< 5\%$) of the radiance count in Ctrl from February 14 to March 6 (Fig. S6). Figure S7 shows a channel peaking at 662 hPa from IASI onboard Metop-A. While the radiance counts and the std of OmB in the two experiments are not significantly different, the amplitude of TBC is slightly smaller (~1.3%) in Ctrl than in Deny, again demonstrating the dropsondes reduced the TBC amplitude required. Results for AIRS channels in the lower- to mid-troposphere show the radiance count is more associated with the std of OmB than the amplitude of TBC (see Fig. S8 for channel 215). Because of the overall small-amplitude TBCs, the variation of radiance count is more sensitive to the variation of OmB change. Stratospheric channels for infrared radiances show negligible differences between Ctrl and Deny (not shown).

4. Same as Fig. 2 but for the CrIS MWIR channel 1022 (WF peaks at 585 hPa).

4 Discussion and Conclusion

Can the dropsonde data collected from Atmospheric River Reconnaissance (AR Recon) affect the assimilation of satellite radiances? If so, how will the impact vary across different satellite types or different channels for a similar satellite type? What mechanism might contribute to the impact? This study has explored answers to these questions by employing data denial experiments for AR Recon 2020 with the Global Data Assimilation System (GDAS) at National Centers for Environmental Predictions. The assimilation of dropsondes can increase the amount of tropospheric radiance data that pass the quality control by 5-10% over the northeastern Pacific and North America (PNA). The most substantial impacts are shown in the all-sky microwave radiances (e.g., AMSU-A channels 1-4 and 15). The increased radiance amount is mainly achieved by the reduced total bias correction amplitude in the experiment Ctrl that assimilated dropsonde data. Improved background and the resultant smaller

12

observation-minus-background have also contributed to the increased number of radiance observations that are used in GDAS. Impacts on hyperspectral infrared sounders in the mid-to lower-troposphere are overall smaller than that for all-sky microwave soundings, and the increased amount of radiance data is more associated with the bias correction procedure for CrIS whereas it is more related to the improved background for the IASI and AIRS channels. Impacts on stratospheric channels for both microwave soundings and the infrared are generally negligible.

High-accuracy RO soundings can anchor satellite data in the stratosphere (Cucurull et al., 2014). The anchoring effects shown in Cucurull et al. (2014) are focused on higher altitudes such as the 10 hPa level. This study examines the anchoring impact of dropsonde profiles at lower altitudes (i.e., from near the surface to 400 hPa), where dropsondes are the dominant conventional observations (Zheng et al., 2021a) and RO soundings have degraded quality and quantity. One notable advantage of RO soundings is its global coverage and availability for all data assimilation cycles. However, our results have shown that even with the limited number of AR Recon flights and relatively localized sampling regions, dropsondes can act as effective anchor data for the PNA region and the Northern Hemisphere, particularly in the lower- to mid-troposphere.

The direct impact of AR Recon dropsonde on forecast skills of numerical weather models has been demonstrated in Zheng et al. (2021). The present study demonstrates their indirect impact on the model analysis and the forecasts by anchoring the assimilation of dropsondes. This study fills a gap in the research on how conventional data can impact the use of remotely-sensed data and help to improve the assimilation of radiance channels in the lowest atmosphere, where most high-impact weather events occur.

AR Recon also produces other observations that can be useful as anchoring data. Drifting buoys measuring sea level pressure and sea surface temperature are deployed during AR Recon to supplement the existing Global Drifter Program buoys. Airborne RO soundings are collected during AR Recon missions (Haase et al., 2021). These observations can provide critical anchor data over a generally data-sparse region. Follow-up work could focused on the impact of such data on radiance assimilation.

Open Research

Satellite observations used in this study can be accessed via UC San Diego Library Digital Collections from https://doi.org/10.6075/J0D21XSQ (Zheng et

al., 2022). The GFS FNL data have been archived at NCAR UCAR Research Data Archive (https://rda.ucar.edu/datasets/ds083.2/).

References

Andersson, E., Bauer, P., Beljaars, A., Chevallier, F., Hólm, E., Janisková, M., Kållberg, P., Kelly, G., Lopez, P., Mcnally, A. and Moreau, E. (2005), Assimilation and modeling of the atmospheric hydrological cycle in the ECMWF forecasting system. *Bulletin of the American Meteorological Society, 86*(3), 387–402. doi: 10.1175/BAMS-86-3-387

Auligné, T., McNally, A.P. and Dee, D.P. (2007), Adaptive bias correction for satellite data in a numerical weather prediction system. *Quarterly Journal of the Royal Meteorological Society, 133*(624), 631–642. doi: 10.1002/qj.56

Aumann, H. H., and Coauthors, 2003: AIRS/AMSU/HSB on the Aqua mission: Design, science objectives, data products, and processing systems. *IEEE Trans. Geosci. Remote Sens., 41*, 253–264. doi: 10.1109/TGRS.2002.808356.

Bauer, P., Lopez, P., Salmond, D., Benedetti, A., Saarinen, S. and Bonazzola, M. (2006), Implementation of 1D+ 4D-Var assimilation of precipitation-affected microwave radiances at ECMWF. II: 4D-Var. *Quarterly Journal of the Royal Meteorological Society, 132*(620), 2307–2332. doi: 10.1256/qj.06.07

Bhargava, K., Kalnay, E., Carton, J.A. and Yang, F. (2018), Estimation of systematic errors in the GFS using analysis increments. *Journal of Geophysical Research: Atmospheres*, *123*(3), 1626–1637. doi: 10.1002/2017JD027423

Bormann, N., Fouilloux, A. and Bell, W. (2013), Evaluation and assimilation of ATMS data in the ECMWF system. *Journal of Geophysical Research: Atmospheres*, *118*(23), 12970–12980. doi: 10.1002/2013JD020325

Boukabara, S.A., Weng, F. and Liu, Q. (2007), Passive microwave remote sensing of extreme weather events using NOAA-18 AMSUA and MHS. *IEEE Transactions on Geoscience and Remote Sensing*, *45*(7), 2228–2246. doi: 10.1109/TGRS.2007.898263

Caplan, P., Derber, J., Gemmill, W., Hong, S.Y., Pan, H.L. and Parrish, D. (1997), Changes to the 1995 NCEP operational medium-range forecast model analysis–forecast system. *Weather and Forecasting*, *12*(3), 581–594.

Chen, J.H., Lin, S.J., Magnusson, L., Bender, M., Chen, X., Zhou, L., Xiang, B., Rees, S., Morin, M. and Harris, L. (2019), Advancements in hurricane prediction with NOAA's next-generation forecast system. *Geophysical Research Letters, 46*(8), 4495–4501. doi: 10.1029/2019GL082410

Collard, A.D. (2007), Selection of IASI channels for use in numerical weather prediction. *Quarterly Journal of the Royal Meteorological Society, 133*(629), 1977–1991. doi: 10.1002/qj.178

Courtier, P., and Coauthors, 1993: Variational assimilation at ECMWF. *ECMWF Tech. Memo. 194*. doi: 10.21957/j7h4sk4ha

Cucurull, L., Anthes, R.A. and Tsao, L.L. (2014). Radio occultation observations as anchor observations in numerical weather prediction models and associated reduction of bias corrections in microwave and infrared satellite observations. *Journal of Atmospheric and Oceanic Technology*, *31*(1), 20–32. doi: 10.1175/JTECH-D-13-00059.1

Dee, D.P. (2004), Variational bias correction of radiance data in the ECMWF system. *Proceedings of the ECMWF Workshop on Assimilation of High Spectral Resolution Sounders in NWP*, Reading, UK, 28 June–1 July, *28,* 97–112. [Available online at https://www.ecmwf.int/sites/default/files/elibrary/2004/8930-variational-bias-correction-radiance-data-ecmwf-system.pdf]

Dee, D.P. and Uppala, S. (2009), Variational bias correction of satellite radiance data in the ERA-Interim reanalysis. *Quarterly Journal of the Royal Meteorological Society*, *135*(644), 1830–1841. doi: 10.1002/qj.493

Derber, J.C.; Wu, W.-S. (1998), The use of TOVS cloud-cleared radiances in the NCEP SSI analysis system. *Monthly Weather Review*, *126*, 2287–2299.

Eresmaa, R., Letertre-Danczak, J., Lupu, C., Bormann, N. and McNally, A.P. (2017), The assimilation of Cross-track Infrared Sounder radiances at ECMWF. *Quarterly Journal of the Royal Meteorological Society*, *143*(709), 3177–3188. doi: 10.1002/qj.3171

Eyre, J.R., G. Kelly, A. P. McNally, E. Andersson, and A. Persson (1993), Assimilation of TOVS radiances through one dimensional variational analysis. *Quarterly Journal of the Royal Meteorological Society*, *119*, 1427–1463. doi: 10.1002/qj.49711951411

Gambacorta, A., and C. D. Barnet, 2013: Methodology and information content of the NOAA NESDIS operational channel selection for the Cross-track Infrared Sounder (CrIS). *IEEE Trans. Geosci. Remote Sens., 51*, 3207–3216. doi: 10.1109/TGRS.2012.2220369.

Geer, A.J. and Bauer, P. (2011). Observation errors in all-sky data assimilation. *Quarterly Journal of the Royal Meteorological Society*, *137*(661), 2024–2037. doi: 10.1002/qj.830

Gershunov, A., Shulgina, T., Ralph, F.M., Lavers, D.A. and Rutz, J.J. (2017), Assessing the climate-scale variability of atmospheric rivers affecting western North America. *Geophysical Research Letters, 44*(15), 7900–7908. doi: 10.1002/2017GL074175

Guan, B. and Waliser, D.E. (2015). Detection of atmospheric rivers: Evaluation and application of an algorithm for global studies. *Journal of Geophysical Research: Atmospheres, 120*(24), 12514–12535. doi: 10.1002/2015JD024257

Haase, J.S., Murphy, M.J., Cao, B., Ralph, F.M., Zheng, M. and Delle Monache,

L. (2021), Multi-GNSS Airborne Radio Occultation Observations as a Complement to Dropsondes in Atmospheric River Reconnaissance. *Journal of Geophysical Research: Atmospheres*, p.e2021JD034865. doi: 10.1029/2021JD034865

Han, Y., and co-authors, (2013), Suomi NPP CrIS measurements, sensor data record algorithm, calibration and validation activities, and record data quality. *Journal of Geophysical Research: Atmospheres, 118*, 12734–12748, doi: 10.1002/2013JD020344

Harris, B.A., and Kelly G. (2001), A satellite radiance-bias correction scheme for data assimilation. *Quarterly Journal of the Royal Meteorological Society, 127*, 1453–1468. doi: 10.1002/qj.49712757418

Healy, S.B. (2008), Assimilation of GPS radio occultation measurements at ECMWF. In *Proceedings of the GRAS SAF Workshop on Applications of GPSRO measurements*, ECMWF, Reading, UK, 99–109.

Hersbach, H., Bell, B., Berrisford, P., Hirahara, S., Horányi, A., Muñoz-Sabater, J., Nicolas, J., Peubey, C., Radu, R., Schepers, D. and Simmons, A., et al. (2020), The ERA5 global reanalysis. *Quarterly Journal of the Royal Meteorological Society, 146*(730), 1999–2049. doi: 10.1002/qj.3803

Hilton F, Atkinson NC, English SJ, Eyre JR. (2009), Assimilation of IASI at the Met Office and assessment of its impact through observing system experiments. *Quarterly Journal of the Royal Meteorological Society, 135*, 495–505. doi: 10.1002/qj.379

Kleist, D.T., Parrish, D.F., Derber, J.C., Treadon, R., Wu, W.S. and Lord, S. (2009), Introduction of the GSI into the NCEP global data assimilation system. *Weather and Forecasting, 24*(6), pp.1691-1705. doi: 10.1175/2009WAF2222201.1

Kleist, D.T. and Ide, K. (2015), An OSSE-based evaluation of hybrid variational–ensemble data assimilation for the NCEP GFS. Part II: 4DEnVar and hybrid variants. *Monthly Weather Review, 143*(2), 452–470. doi: 10.1175/MWR-D-13-00350.1

Lavers, D.A., Rodwell, M.J., Richardson, D.S., Ralph, F.M., Doyle, J.D., Reynolds, C.A., Tallapragada, V. and Pappenberger, F. (2018), The gauging and modeling of rivers in the sky. *Geophysical Research Letters, 45*(15), 7828–7834. doi: 10.1029/2018GL079019

Li, X., Zou, X. and Zeng, M. (2019), An alternative bias correction scheme for CrIS data assimilation in a regional model. *Monthly Weather Review, 147*(3), 809–839. doi: 10.1175/MWR-D-18-0044.1

Liu, Z., Schwartz, C.S., Snyder, C. and Ha, S.Y. (2012), Impact of assimilating AMSU-A radiances on forecasts of 2008 Atlantic tropical cyclones initialized with a limited-area ensemble Kalman filter. *Monthly Weather Review, 140*(12), 4017–4034. doi: 10.1175/MWR-D-12-00083.1

Maier, M.W., Gallagher III, F.W., St. Germain, K., Anthes, R., Zuffada, C.,

Menzies, R., Piepmeier, J., Di Pietro, D., Coakley, M.M. and Adams, E. (2021), Architecting the Future of Weather Satellites. *Bulletin of the American Meteorological Society*, *102*(3), E589–E610. doi: 10.1175/BAMS-D-19-0258.1

Majumdar, S.J., 2016. A review of targeted observations. *Bulletin of the American Meteorological Society, 97*(12), 2287–2303. doi: 10.1175/BAMS-D-14-00259.1

McNally, A.P., Watts, P.D., A. Smith, J., Engelen, R., Kelly, G.A., Thépaut, J.N. and Matricardi, M. (2006), The assimilation of AIRS radiance data at ECMWF. *Quarterly Journal of the Royal Meteorological Society, 132*(616), 935–957. doi: https://doi.org/10.1256/qj.04.171

Mo, T., 2011. Calibration of the NOAA AMSU-A radiometers with natural test sites. *IEEE transactions on geoscience and remote sensing, 49*(9), 3334–3342. doi: 10.1109/MICRORAD.

2010.5559548

Ota, Y., Derber, J.C., Kalnay, E. and Miyoshi, T. (2013), Ensemble-based observation impact estimates using the NCEP GFS. *Tellus A: Dynamic Meteorology and Oceanography, 65*(1), 20038. doi: 10.3402/tellusa.v65i0.20038

Otkin, J.A., Potthast, R. and Lawless, A.S. (2018). Nonlinear bias correction for satellite data assimilation using Taylor series polynomials. *Monthly Weather Review, 146*(1), 263–285. doi: 10.1175/MWR-D-17-0171.1

Posselt, D.J., Stephens, G.L., and Miller, M. (2008), CloudSat: Adding a new dimension to a classical view of extratropical cyclones. *Bulletin of the American Meteorological Society, 89*(5), 599–610. doi: https://doi.org/10.1175/BAMS-89-5-599

Pu, Z., Li, X., Velden, C.S., Aberson, S.D. and Liu, W.T. (2008), The impact of aircraft dropsonde and satellite wind data on numerical simulations of two landfalling tropical storms during the tropical cloud systems and processes experiment. *Weather and Forecasting, 23*(1), 62–79. doi: https://doi.org/10.1175/2007WAF2007006.1

Rao, P. K., S. J. Holmes, R. K. Anderson, J. S. Winston, and P. E. Lehr, Eds., (1990), Weather Satellites: Systems, Data, and Environmental Applications. *Amer. Meteor. Soc.*, 473 pp.

Ralph, F. M., P. J. Neiman, G. A. Wick, and C. S. Velden (2004), Satellite and CALJET aircraft observations of atmospheric rivers over the eastern North Pacific Ocean during the winter of 1997/98. *Monthly weather review, 132*, 1721–1745. doi: 10.1175/1520-0493(2004)132%3C1721:SACAOO%3E2.0.CO;2

Ralph, F.M., Neiman, P.J. and Rotunno, R. (2005), Dropsonde observations in low-level jets over the northeastern Pacific Ocean from CALJET-1998 and PACJET-2001: Mean vertical-profile and atmospheric-river characteris-tics. *Monthly weather review, 133*(4), 889–910. doi: 10.1175/MWR2896.1

Ralph, F.M., Iacobellis, S.F., Neiman, P.J., Cordeira, J.M., Spackman, J.R., Waliser, D.E., Wick, G.A., White, A.B. and Fairall, C. (2017), Dropsonde observations of total integrated water vapor transport within North Pacific atmospheric rivers. *Journal of Hydrometeorology, 18*(9), 2577–2596. doi: 10.1175/JHM-D-17-0036.1

Ralph, F.M., Cannon, F., Tallapragada, V., Davis, C.A., Doyle, J.D., Pappenberger, F., Subramanian, A., Wilson, A.M., Lavers, D.A., Reynolds, C.A. and Haase, J.S. (2020). West Coast forecast challenges and development of atmospheric river reconnaissance. *Bulletin of the American Meteorological Society, 101*(8), E1357–E1377. doi: 10.1175/BAMS-D-19-0183.1

Reynolds, C.A., Doyle, J.D., Ralph, F.M., and Demirdjian R. (2019), Adjoint sensitivity of North Pacific atmospheric river forecasts. *Monthly Weather Review*, 147(6), 1871–1897. doi: 10.1175/MWR-D-18-0347.1

Rosenkranz, P.W. (2001), Retrieval of temperature and moisture profiles from AMSU-A and AMSU-B measurements. *IEEE Transactions on Geoscience and Remote Sensing, 39*(11), 2429–2435. doi: 10.1109/36.964979.

Stone, R.E., Reynolds, C.A., Doyle, J.D., Langland, R.H., Baker, N.L., Lavers, D.A. and Ralph, F.M. (2020), Atmospheric river reconnaissance observation impact in the Navy global forecast system. *Monthly Weather Review, 148*(2), pp.763-782. doi: 10.1175/MWR-D-19-0101.1

Stuart, A., Ord, K., and Arnold, S. (2004), Kendall's Theory of Statistics. 6th edition, Volume 2A, Chapter 28, Wiley, 2004.

Tong, M., Zhu, Y., Zhou, L., Liu, E., Chen, M., Liu, Q. and Lin, S.J. (2020), Multiple hydrometeors all-sky microwave radiance assimilation in FV3GFS. *Monthly Weather Review, 148*(7), 2971–2995. doi: 10.1175/MWR-D-19-0231.1

Wang, X. and Lei, T. (2014). GSI-based four-dimensional ensemble–variational (4DEnsVar) data assimilation: Formulation and single-resolution experiments with real data for NCEP Global Forecast System. *Monthly Weather Review, 142*(9), pp.3303-3325. doi: 10.1175/MWR-D-13-00303.1

Weng, F. (2007), Advances in radiative transfer modeling in support of satellite data assimilation, *Journal of the Atmospheric Sciences, 64*, 3799–3807. doi:10.1175/2007JAS2112.1.

Wu, W.S., Purser, R.J., and Parrish D.F. (2002), Three-dimensional variational analysis with spatially inhomo-geneous covariances. *Monthly Weather Review*, 130, 2905–2916.

Yang, F., and Tallapragada, V. (2018), Evaluation of Retrospective and Real-time NGGPS FV3GFS Experiments for Q3FY18 Beta Implementation. Paper presented at *25th Conference on Numerical Weather Prediction, American Meteorological Society*, Denver, Colorado. [Available online at https://ams.confex .com/ams/29WAF25NWP/webprogram/Paper345231.html]

Zhang, Z., Ralph, F.M. and Zheng, M. (2019), The relationship between extratropical cyclone strength and at-mospheric river intensity and position. *Geophysical Research Letters, 46*(3), 1814–1823. doi: 10.1029/2018GL079071

Zheng, M., Chang, E.K. and Colle, B.A. (2019), Evaluating US East Coast winter storms in a multimodel ensemble using EOF and clustering approaches. *Monthly Weather Review, 147*(6), 1967–1987. doi: 10.1175/MWR-D-18-0052.1

Zheng, M., Delle Monache, L., Wu, X., Ralph, F.M., Cornuelle, B., Tallapragada, V., Haase, J.S., Wilson, A.M., Mazloff, M., Subramanian, A. and Cannon, F. (2021a). Data gaps within atmospheric rivers over the northeastern Pacific. *Bulletin of the American Meteorological Society, 102*(3), E492–E524. doi: 10.1175/BAMS-D-19-0287.1

Zheng, M., Delle Monache, L., Cornuelle, B.D., Ralph, F.M., Tallapragada, V.S., Subramanian, A., Haase, J.S., Zhang, Z., Wu, X., Murphy, M.J. and Higgins, T.B. (2021b), Improved Forecast Skill through the Assimilation of Dropsonde Observations from the Atmospheric River Reconnaissance Program. *Journal of Geophysical Research: Atmospheres*, p.e2021JD034967. doi: 10.1029/2021JD034967

Zheng, Minghua; Delle Monache, Luca; Wu, Xingren; Kawzenuk, Brian; Ralph, F. Martin; Zhu, Yanqiu; Torn, Ryan; Tallapragada, Vijay S.; Zhang, Zhenhai; Wu, Keqin (2022). Data from: Impact of Atmospheric River Reconnaissance Dropsonde Data on the Assimilation of Satellite Data in GFS. *UC San Diego Library Digital Collections.* https://doi.org/10.6075/J0D21XSQ

Zhu, Y. and Newell, R.E. (1994), Atmospheric rivers and bombs. *Geophysical Research Letters, 21*(18), 1999–2002. doi: 10.1029/94GL01710

Zhu, Y., Derber, J., Collard, A., Dee, D., Treadon, R., Gayno, G. and Jung, J.A. (2014a), Enhanced radiance bias correction in the National Centers for Environmental Prediction's Gridpoint Statistical Interpolation data assimilation system. *Quarterly Journal of the Royal Meteorological Society, 140*(682), 1479–1492. doi: 10.1002/qj.2233

Zhu, Y., Derber, J., Collard, A., Dee, D., Treadon, R., Gayno, G., Jung, J.A., Groff, D., Liu, Q., Delst, P. and Liu, E. (2014b), Variational bias correction in the NCEP's data assimilation system. Paper presented at *19th International TOVS Study Conference*, Jeju Island, South Korea. [Available online at http://cimss.ssec.wisc.edu/itwg/itsc/itsc19/program/papers/10_02_zhu.pdf.]

Zhu, Y., Liu, E., Mahajan, R., Thomas, C., Groff, D., Van Delst, P., Collard, A., Kleist, D., Treadon, R. and Derber, J.C. (2016), All-sky microwave radiance assimilation in NCEP's GSI analysis system. *Monthly Weather Review, 144*(12), 4709–4735. doi: 10.1175/MWR-D-15-0445.1